THE JOURNAL OF BIOLOGICAL CHEMISTRY VOL. 284, NO. 33, pp. 22133–22139, August 14, 2009

Tetramerization and Cooperativity in *Plasmodium falciparum* Glutathione *S*-Transferase Are Mediated by Atypic Loop 113–119

Received for publication, April 30, 2009 Published, JBC Papers in Press, June 16, 2009, DOI 10.1074/jbc.M109.015198

Eva Liebau[‡1], Kutayba F. Dawood[§1], Raffaele Fabrini[§1], Lena Fischer-Riepe[‡], Markus Perbandt[¶‖], Lorenzo Stella[§], Jens Z. Pedersen[**], Alessio Bocedi[‡‡§§], Patrizia Petrarca[**], Giorgio Federici[¶¶], and Giorgio Ricci[§2]

*From the [‡]Institute of Animal Physiology, University of Münster, Hindenburgplatz, 55 Münster, Germany, the Departments of [§]Chemical Sciences and Technologies and **Biology, University of Rome "Tor Vergata," 00133 Rome, Italy, the [¶]Institute of Biochemistry, Center for Structural and Cell Biology, University of Luebeck, Ratzeburger Allee 160, 23538 Luebeck, Germany, the [‖]Laboratory for Structural Biology of Infection and Inflammation, Deutsches Elektronen Synchrotron, Notkestrasse 85, 22603 Hamburg, Germany, the [‡‡]Department of Biology, University of Rome "Roma Tre," 00146 Rome, Italy, the [§§]Department of Molecular Genetics and Microbiology, Duke University, Durham, North Carolina 27708, and the [¶¶]Children's Hospital "Bambin Gesù," 00165 Rome, Italy*

Glutathione *S*-transferase of *Plasmodium falciparum* (*Pf*GST) displays a peculiar dimer to tetramer transition that causes full enzyme inactivation and loss of its ability to sequester parasitotoxic hemin. Furthermore, binding of hemin is modulated by a cooperative mechanism. Site-directed mutagenesis, steady-state kinetic experiments, and fluorescence anisotropy have been used to verify the possible involvement of loop 113–119 in the tetramerization process and in the cooperative phenomenon. This protein segment is one of the most prominent structural differences between *Pf*GST and other GST isoenzymes. Our results demonstrate that truncation, increased rigidity, or even a simple point mutation of this loop causes a dramatic change in the tetramerization kinetics that becomes at least 100 times slower than in the native enzyme. All of the mutants tested have lost the positive cooperativity for hemin binding, suggesting that the integrity of this peculiar loop is essential for intersubunit communication. Interestingly, the tetramerization process of the native enzyme that occurs rapidly when GSH is removed is prevented not only by GSH but even by oxidized glutathione. This result suggests that protection by *Pf*GST against hemin is independent of the redox status of the parasite cell. Because of the importance of this unique segment in the function/structure of *Pf*GST, it could be a new target for the development of antimalarial drugs.

Approximately two million deaths in the world per year are caused by *Plasmodium falciparum*, the parasite responsible for tropical malaria (1, 2). In the last years, increasing interest has been developing for the peculiar glutathione *S*-transferase (*Pf*GST)[3] expressed by this parasite. Expressed in almost all living organisms, GSTs represent a large superfamily of multifunctional detoxifying enzymes that are able to conjugate GSH to a lot of toxic electrophilic compounds, thus facilitating their excretion. Many other protection roles of GSTs have been described, including the enzymatic reduction of organic peroxides (3–5), the inactivation of the proapoptotic JNK through a GST·JNK complex (6), and the protection of the cell from excess nitric oxide (7). The mammalian cytosolic GSTs are dimeric proteins grouped into eight species-independent classes termed Alpha, Kappa, Mu, Omega, Pi, Sigma, Theta, and Zeta on the basis of sequence similarity, immunological reactivity, and substrate specificity (3, 8–11). *Pf*GST is one of the most abundant proteins expressed by *P. falciparum* (from 1 to 10%, *i.e.* from 0.1 to 1 mM) (12), and different from what occurs in many organisms, it is the sole GST isoenzyme expressed by this parasite. Despite its structural similarity to the Mu class GST, this specific isoenzyme cannot be assigned to any known GST class (13). The interest in this enzyme is due to its particular protective role in the parasite. In fact, in addition to the usual GST activity that promotes the conjugation of GSH to electrophilic centers of toxic compounds, this protein efficiently binds hemin, and thus it could protect the parasite (that resides in the erythrocytes) from the parasitotoxic effect of this heme by-product (14). Specific compounds that selectively inhibit its catalytic activity or hemin binding could be promising candidates as antimalarial drugs. In this context, the discovery of structural or mechanistic properties of this enzyme that are not found in other GSTs may be important for designing selective inhibitors that are toxic to the parasite but harmless for the host cells. Two properties never observed in other members of the GST superfamily are of particular interest. The first property is that this enzyme, in the absence of GSH, is inactivated in a short time and loses its ability to bind hemin (15). Recent studies indicated that the inactivation process is related to a dimer to tetramer transition (13, 16, 17). The second property is the strong positive homotropic phenomenon that modulates the affinity of the two subunits for hemin (15). The x-ray crystal structure of *Pf*GST, solved by two different groups (13, 18), provides insights into this effect. From a structural point of view, the most intriguing differences of *Pf*GST when compared with other GSTs are a more solvent-exposed H-site and an atypic extra loop connecting helix α-4 and helix α-5 (residues

[1] These authors equally contributed to this work.
[2] To whom correspondence should be addressed: via della Ricerca Scientifica, 1, 00133 Rome, Italy. Tel.: 390672594379; Fax: 3972594328; E-mail: riccig@uniroma2.it.
[3] The abbreviations used are: *Pf*GST, glutathione *S*-transferase from *P. falciparum*; JNK, c-Jun N-terminal kinase.

113–119; see also Fig. 1) that could be involved in the dimer-dimer interaction. Actually, in the absence of ligands, two biological dimers form a tetramer, and these homodimers are interlocked with each other by loop 113–119 of one homodimer, which occupies an H-site of the other homodimer (13, 18). Upon binding of *S*-hexylglutathione, loop 113–119 rearranges; residues Asn-114, Leu-115, and Phe-116 form an additional coil in helix α-4; and the side chains of Asn-111, Phe-116, and Tyr-211 flip into the H-site of the same dimer (17, 18). The changed course of residues 113–119 in the liganded enzyme prevents the interlocking of the dimers.

In this paper, by means of site-directed mutagenesis, fluorescence anisotropy, kinetic studies, and size exclusion chromatography, we check the influence of selected mutations of this atypic loop in the tetramerization process and the possible involvement of this protein segment in the cooperative phenomenon that characterizes hemin binding. In addition we describe that the tetramerization process is inhibited not only by GSH but even by GSSG. This finding suggests that hemin binding of *Pf*GST is independent of the redox status of the cell. Finally, we demonstrate that the presence of GSH (or GSSG) in the active site is not essential for hemin binding, but this interaction only requires an active dimeric conformation.

EXPERIMENTAL PROCEDURES

Materials—GSH, 1-chloro-2,4-dinitrobenzene, GSSG, and hemin were obtained from Sigma-Aldrich.

In Vitro Site-directed Mutagenesis—*Pf*GST mutants were generated using the commercial QuikChange® site-directed mutagenesis kit (Stratagene, La Jolla, CA) according to the manufacturer's instructions. The basic procedure utilized the purified expression vector pJC20 containing the complete cDNA of the *Pf*GST as an insert (18) and two synthetic oligonucleotide primers designed to introduce the proper mutations. In mutant A, the flexibility of the loop region was lowered by the substitution of Thr-113 and Asn-119 by two prolines. For the generation of mutant A, the mutagenesis primer 5′-TATAAATTTAATAATCCCAATTTATTTAAACAACCTGAAACAACTTTTTTA-3′ and the respective primer complementary to the opposite strand were used. For mutant B, the single point mutation Q118A was carried out using the primer 5′-ACCAATTTATTTAAAGCGAATGAAACAACTTTT-3′ and the complementary primer on the other strand. Finally, in mutant C, the entire loop region was replaced by two alanine residues using the primer 5′-CAGGATATTCATTATAAATTTAATAATACCGCAGCAAATGAAACAACTTTTTTAAATGAG-3′ and the respective complementary primer. The entire coding region was sequenced to ensure the presence of the desired mutation and the absence of undesired alterations in the *Pf*GST coding region.

Recombinant Expression and Purification of Wild-type PfGST and Mutants—Expression and purification of the three mutants were carried out as described previously for the wild-type enzyme (19, 20). Briefly, after transformation of pJC20-*Pf*GST into *Escherichia coli* BL21(DE3) pLys, bacterial cells were grown overnight in Luria-Bertani medium containing 50 μg/ml ampicillin. This stock culture was diluted 1:100 in the same medium, and then the bacteria were grown to an A_{600} of 0.5 before induction with 1 mM of isopropyl β-D-thiogalactoside. After 3 h at 37 °C, bacterial cells were harvested by centrifugation, and the bacterial pellet was resuspended in phosphate-buffered saline (150 mM NaCl, 16 mM Na_2HPO_4, 4 mM NaH_2PO_4, pH 7.3) and sonicated. The cell lysate was centrifuged at 100,000 × *g* (1 h, 4 °C). In a batch purification, the supernatant was mixed with glutathione-Sepharose affinity matrix (GE Healthcare). After an overnight incubation at 4 °C followed by washing with 10 bed volumes of phosphate-buffered saline, the recombinant protein was eluted with 15 mM GSH in 50 mM Tris-HCl, pH 7.2. The purity of the eluted proteins was checked by SDS-PAGE. The purified forms of *Pf*GSTs were stored at −80 °C in the presence of 10 mM GSH. Under these conditions, the enzymes were stable for weeks. Protein concentrations were calculated assuming an A_{280} of 1.1 for 1 mg/ml for *Pf*GSTs on the basis of the amino acid sequence (21). A molecular mass of 25 kDa/GST subunit was used in the calculation (19).

Human GST Expression and Purification—Human GSTA1-1 (Alpha class), GSTM2-2 (Mu class), and GSTP1-1 (Pi class) were expressed in *E. coli* and purified as described previously (22–24).

Enzymatic Activity—Standard *Pf*GST (wild type and mutants) and human GST (Alpha, Pi, and Mu classes) activities were measured at 25 °C in a 0.1 M potassium phosphate buffer, pH 6.5, containing 1 mM GSH and 1 mM 1-chloro-2,4-dinitrobenzene. The activity was assayed spectrophotometrically by following the enzymatic product at 340 nm (ϵ = 9600 M^{-1} cm^{-1}). The values of k_{cat} were calculated at saturating GSH concentrations and 1 mM 1-chloro-2,4-dinitrobenzene.

Sephadex G-25 Chromatography—Gel filtration was carried out on a Sephadex G-25 column (GE Healthcare) to remove the storage GSH (10 mM). The column was equilibrated and run with 10 mM potassium phosphate buffer, pH 7.2, with a flow rate of 1 ml/min at 25 °C. To verify whether GSSG prevents the enzyme tetramerization, the column was equilibrated and run with the above-mentioned buffer containing 1 mM GSSG. Protein samples without GSH (1 mg/ml native *Pf*GST or mutants) were incubated at 25 °C and assayed at fixed times for enzyme inactivation and tetramerization (see below).

Anisotropy Experiments—Fluorescence anisotropy experiments were performed with a Spex Fluoromax 2 fluorometer, using 280 nm excitation, 335 nm emission, and a 295-nm cut-off filter in the emission channel. The means ± S.D. of anisotropy values were calculated from nine replicate experiments. 0.124 mg/ml protein concentration was employed in all experiments, and the effect of substrate binding was monitored by adding 1 mM GSH.

Size Exclusion Chromatography—Gel filtration experiments were performed using a Superdex® 200 HR 10/30 column on an LKB fast protein liquid chromatography system (GE Healthcare). The column was equilibrated with 10 mM potassium phosphate buffer, pH 7.2, and calibrated with the following proteins: cytochrome *c* (12 kDa), ovalbumin (43 kDa), serum albumin (67 kDa), transferrin (81 kDa), and glucose oxidase (160 kDa). The experiments were carried out at room temperature at a flow rate of 1 ml/min.

Inhibition of PfGSTs by Hemin—Fresh hemin stock solutions were prepared as described previously (15). Inhibition of *Pf*GSTs by hemin was studied by adding variable amounts of hemin (from 0.2 to 10 μM) with a fixed enzyme concentration (1 μM) in 1 ml of 0.1 M potassium phosphate buffer, pH 6.5, at 25 °C. After 10 s, 1 mM GSH and 1 mM 1-chloro-2,4-dinitrobenzene were added for activity measurements, followed by absorption at 340 nm. The data obtained by varying hemin concentrations were analyzed using the Hill equation (Equation 1),

$$v_i/v_{max} = [S]^n/(K^n + [S]^n) \quad \text{(Eq. 1)}$$

where v_i is the initial velocity observed at a given concentration of hemin, v_{max} is the velocity observed in the absence of inhibitor, [S] is the hemin concentration, and n is the Hill coefficient at the hemin concentration corresponding to half-enzyme saturation.

The inhibition data were also analyzed with a two-site Adair model for ligand binding to a homodimeric macromolecule to estimate K_1 (low affinity) and K_2 (high affinity) constants for hemin binding,

$$v_i/v_{max} = ([S]/K_1 + [S]^2/\alpha K_1^2)/(1 + 2[S]/K_1 + [S]^2/\alpha K_1^2) \quad \text{(Eq. 2)}$$

where K_1 is the dissociation equilibrium constant for hemin binding to the free enzyme, αK_1 (which equals K_2) represents the dissociation equilibrium constant for hemin binding to the monoligated enzyme, and α is the nondimensional interaction parameter coupling the two functionally linked hemin-binding sites.

Isothermic Binding of PfGSTs and Hemin—Isothermic binding of hemin to *Pf*GSTs (1 μM) was measured in a single photon-counting spectrofluorometer (Spex Fluoromax 2 fluorometer) with a sample holder thermostatted at 25 °C. Excitation was at 295 nm, and emission was measured at 333 nm. The affinity of *Pf*GSTs for hemin was determined by measuring the quenching of the intrinsic fluorescence of the protein following the addition of hemin (from 0.1 to 10 μM) in the presence or absence of GSH (or GSSG) in 0.1 M potassium phosphate buffer, pH 6.5. Fluorescence data were corrected both for dilution and inner filter effects. The data were analyzed by the noncooperative Langmuir isotherm equation (Equation 3),

$$\vartheta = \frac{K_D + [\text{hemin}] + [\text{GST}] - \sqrt{(K_D + [\text{hemin}] + [\text{GST}])^2 - 4[\text{hemin}][\text{GST}]}}{2[\text{GST}]} \quad \text{(Eq. 3)}$$

where ϑ (fraction of occupied sites) was determined according to Equation 4,

$$\vartheta = (I - I_0)/(I_{sat} - I_0) \quad \text{(Eq. 4)}$$

where I_0, I, and I_{sat} are the fluorescence intensities observed in the absence of hemin, at each hemin concentration, and at saturation, respectively.

RESULTS AND DISCUSSION

Kinetic Properties of Loop 113–119 Mutants—Selected mutations of *Pf*GST have been designed to evaluate the importance of the native structure/sequence of loop 113–119 in the tetramerization process and in the cooperative phenomenon. In particular, in mutant C, the entire protein segment 113–119 was replaced by two alanine residues; mutant B displays the single point mutation Q118A; and in mutant A, residues Thr-113 and Asn-119 have been substituted by two prolines to lower the flexibility of this protein segment (Fig. 1*A*). Expression and purification of these mutant enzymes in *E. coli* are described under "Experimental Procedures." The three enzymes were analyzed under steady-state kinetic conditions. As shown in Table 1, mutant B and mutant C display kinetic parameters very similar to those of the native enzyme. Surprisingly, the hinge-blocked enzyme (mutant A) reveals approximately four times higher K_m for GSH and approximately three times increased k_{cat}. This decreased affinity for GSH is unexpected because the loop does not interact directly with the G-site.

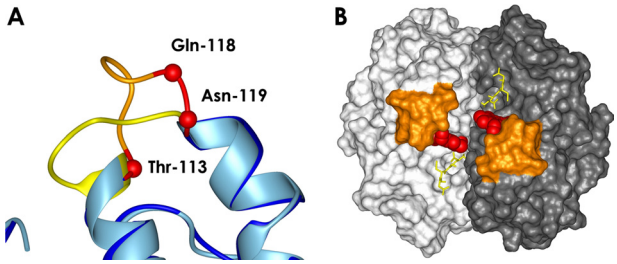

FIGURE 1. *A*, structural changes of loop 113–119 occurring in the dimer (*light blue model* and *yellow loop*; Protein Data Bank code 2AAW) to tetramer (*blue model* and *orange loop*; Protein Data Bank code 1OKT) transition. *Red spheres* indicate the amino acids replaced in this study to obtain mutants A, B, and C. *B*, model of hemin·*Pf*GST complex obtained by docking simulation using the crystal structure for Protein Data Bank code 1Q4J (15). Hemin is shown in *red*, loop 113–119 is in *orange*, and GSH is shown as *yellow sticks*.

TABLE 1

Kinetic parameters of wild-type and mutant *Pf*GSTs

The data shown are the means ± S.D. of three independent determinations.

*Pf*GST	K_m^{GSH}	k_{cat}^{GSH}	k_{cat}^{GSH}/K_m^{GSH}
	mM	s^{-1}	$M^{-1}\,s^{-1}$
Wild-type	0.15 ± 0.02(100%)	0.151 ± 0.007	1000 ± 140
Mutant A (hinge-blocked)	0.61 ± 0.05(406%)	0.413 ± 0.009	680 ± 60
Mutant B (point mutation)	0.20 ± 0.02(137%)	0.122 ± 0.005	610 ± 60
Mutant C (mini loop)	0.17 ± 0.02(114%)	0.160 ± 0.009	940 ± 120

Loop 113–119 Modulates the Kinetics of the Inactivation/Tetramerization Process—Native *Pf*GST loses most of its original activity when incubated at 25 °C in the absence of GSH (Fig. 2*A*). As shown previously, the inactivation seems to be a biphasic event with a first phase that ends at ~50% of native activity and is characterized by an apparent half-time of 3–4 min (15). Even slight perturbations of loop 113–119 dramatically influence the kinetics of the spontaneous inactivation process. In particular all of these mutants retain their original activity after GSH is removed by a Sephadex G-25 column, whereas the native enzyme immediately undergoes ~50% inactivation (Fig. 2*A*). Even after 24 h all of the mutants still display 70–80% of the original activity, whereas the wild-type enzyme is almost completely inactivated. Thus, in these mutants the inactivation process becomes at least 100 times slower than in the native enzyme. Recent studies based on gel filtration experiments have demonstrated that the inactivation caused by the absence of GSH is coupled to a tetramerization process (16, 18). This

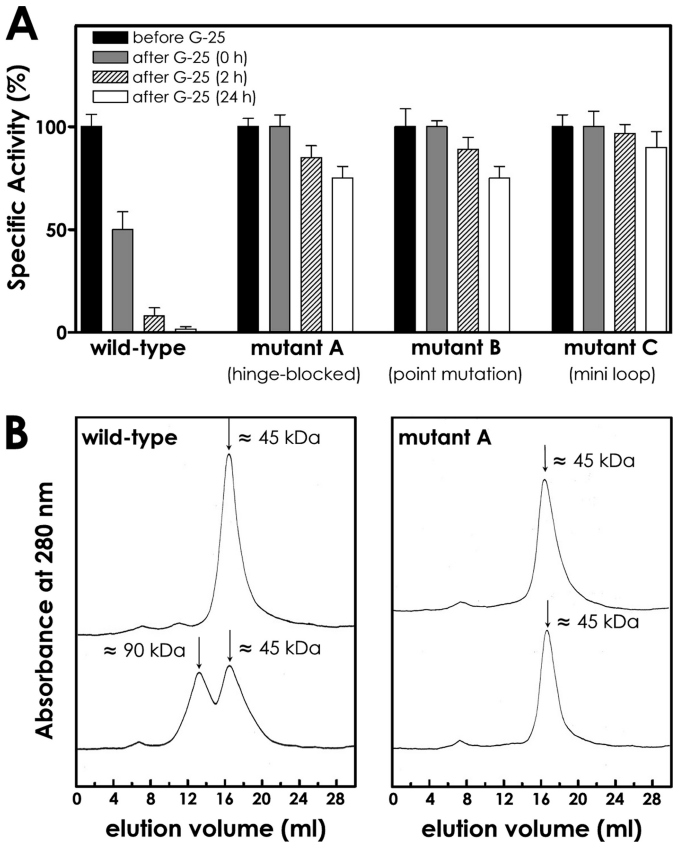

FIGURE 2. **Tetramerization/inactivation of native and mutated *Pf*GSTs in the absence of GSH.** Active dimeric *Pf*GSTs (with 10 mM GSH) were passed through a Sephadex G-25 column. After GSH removal, the enzymes were incubated at 25 °C at a concentration of ~1 mg/ml. *A*, enzymatic activity, assayed at different incubation times (25 °C) after GSH removal. Activity was assayed as described under "Experimental Procedures." *B*, size exclusion chromatography performed on wild-type *Pf*GST and mutant A in the presence of 10 mM GSH (*upper curves*) and immediately after GSH removal by a Sephadex G-25 column (*lower curves*). Very similar results have been found with mutant B and mutant C (data not shown).

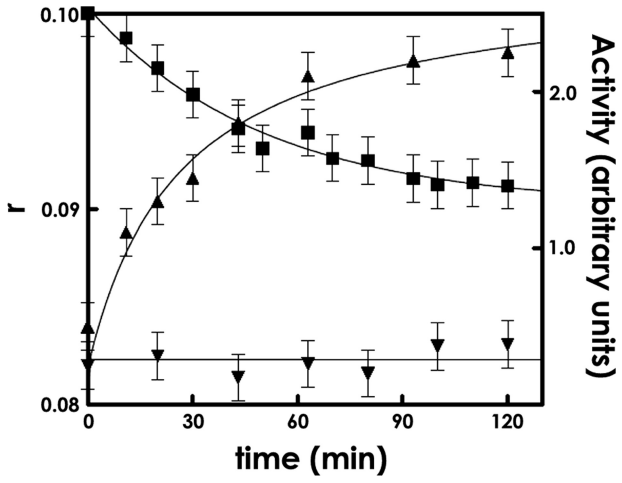

FIGURE 3. **GSH-induced tetramer/dimer transition.** Inactive tetrameric wild-type *Pf*GST (5 μM) obtained by 12 h of incubation in the absence of GSH was incubated with 1 mM GSH in 0.1 M potassium phosphate buffer, pH 6.5, at 25 °C. At fixed times, fluorescence anisotropy (*r*) (■) and enzymatic activity (▲) were monitored. As a control, changes of fluorescence anisotropy of mutant A (incubated for 12 h in the absence of GSH and then treated with 1 mM GSH) are also reported (▼). Mutants B and C (data not shown) display the same behavior as mutant A. The standard deviations of anisotropy values were calculated from nine replicate experiments.

event is reversible and occurs within the GSH concentration range of 0–0.7 mM (16). The persistence of the original activity for our mutants in the absence of GSH (Fig. 2*A*) suggests that the tetramerization is a very slow process for these enzymes or alternatively that they generate an active tetramer. Gel filtration experiments clarified this question. In fact, the native enzyme in the presence of 10 mM GSH shows a single peak corresponding to a molecular mass of a dimeric structure (~45 kDa; Fig. 2*B*). Immediately after the GSH removal through Sephadex G-25 chromatography, ~50% of the enzyme acquires a tetrameric structure. On the contrary, in the same conditions, mutants A and B retain all of their original activity and remain as dimeric proteins (Fig. 2*B*). After incubation for 12 h at 25 °C in the absence of GSH, the native enzyme is almost fully inactivated and mainly in the tetrameric state, whereas mutants A and B formed less than 15% of tetrameric structures (data not shown). Even fewer tetrameric structures have been found for mutant C. Thus, any perturbation of the native sequence in loop 113–119 drastically slows down the tetramerization/inactivation process.

Tetramerization and Inactivation Are Synchronous Events—It is not clear whether the tetramerization of *Pf*GST observed in the absence of GSH is synchronous to the inactivation process or whether these events occur with different kinetics. This detail could be important to define whether tetramerization is the cause or the effect of the loss of activity. Thus, the kinetics of tetramer to dimer transition triggered by GSH binding was studied by means of steady-state fluorescence anisotropy experiments and compared with the reactivation kinetics. An attempt to follow the reverse reaction, *i.e.* the dimer to tetramer transition after removal of GSH, was unsuccessful because of the very fast inactivation of this enzyme in the absence of GSH (15). Steady-state fluorescence anisotropy represents a useful approach for following a dimer/tetramer transition because it provides a measure of the rotational motions of macromolecules (25). Dissociation of a multimer results in a decrease in the fluorescence anisotropy value (*r*), because of the increase in rotational diffusion. In the case of the native *Pf*GST, the starting enzyme is represented by the inactivated enzyme (tetrameric state) obtained after Sephadex G-25 chromatography and subsequent incubation at 25 °C for 12 h in the absence of GSH. Incubation of this inactive enzyme with 1 mM GSH resulted in a decrease of the anisotropy values, accompanied by the parallel recovery of enzymatic activity (Fig. 3). The kinetics of the two processes could be fitted with the same first order kinetics, with a lifetime of 40 min, indicating a strict correlation between the two phenomena but no temporal priority. Mutants A, B, and C, incubated for 12 h without GSH, were slightly inactivated, and as expected, no appreciable change of anisotropy was visible upon incubation with 1 mM GSH (Fig. 3). These data confirm that even a single point mutation in the loop 113–119 region is sufficient to prevent the rapid formation of an inactive tetramer species.

GSSG Inhibits the Tetramerization Process—A surprising property of *Pf*GST is represented by its high affinity for GSSG. From kinetic inhibition experiments, an apparent K_D value of 0.07 mM has been found for GSSG, a value even smaller than that for GSH (0.15 mM). GSSG behaves like a pure competitive inhibitor, indicating that the site of binding must be identified

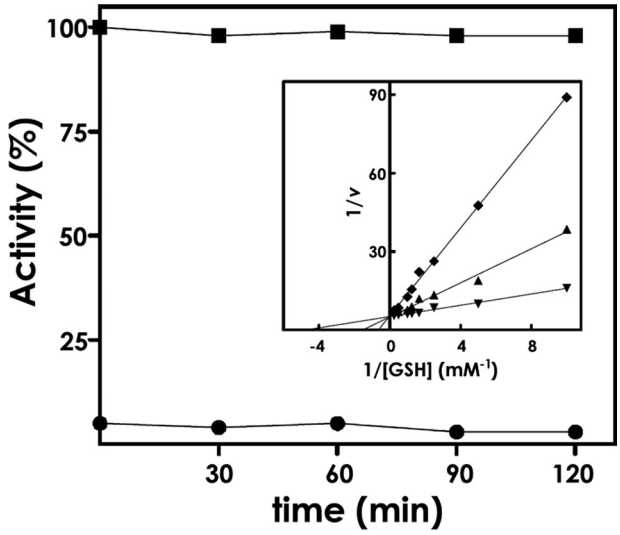

FIGURE 4. **Effects of GSSG on *Pf*GSTs.** ■, active native *Pf*GST (2 mg) was passed through a Sephadex G-25 column saturated with 1 mM GSSG in 10 mM potassium phosphate buffer, pH 7.2, at 25 °C. The specific activity of enzyme was measured at different times at 25 °C. ●, inactivated *Pf*GST tetramer (2 mg) was incubated at 25 °C with 10 mM GSSG. *Inset*, Lineweaver-Burk plot of 1/*v versus* 1/[GSH] obtained by adding variable amounts of GSH (from 0.1 to 4 mM) to the native *Pf*GST in the presence of fixed GSSG concentrations (◆, 0.53 mM; ▲, 0.23 mM; and ▼, 0.03 mM) in 1 ml of 0.1 M potassium phosphate buffer, pH 6.5 (25 °C).

as the G-site (Fig. 4, *inset*). Of particular interest is the influence of GSSG on the inactivation/tetramerization process. As shown in Fig. 4 the presence of GSSG (from 0.1 to 1 mM) prevents the inactivation process, thus stabilizing the dimeric structure. This means that *in vivo* the enzyme should be able to retain its active conformation even when GSH is partially oxidized to GSSG, *i.e.* under oxidative stress. On the other hand, the inactive tetrameric enzyme does not restore its active conformation when incubated with 10 mM GSSG (Fig. 4), indicating that GSSG has limited access to the G-sites in the tetrameric structure. As confirmation, no decrease in anisotropy has been found after the addition of GSSG to the inactive form (data not shown).

*The Integrity of Loop 113–119 Is Crucial for the Positive Cooperativity in Hemin Binding—Pf*GST displays homotropic behavior for hemin binding, so the affinity of the vacant subunit increases approximately 20 times when one hemin molecule binds to the first subunit of the dimer (15). This mechanism has been interpreted as a way to optimize the interception of hemin by the parasite that metabolizes large amounts of host cell hemoglobin and is continuously exposed to this toxic by-product. Other GSTs (Alpha, Mu, and Pi classes) equally able to bind hemin display a noncooperative interaction (Table 2). *Pf*GST mutants make it possible to check the importance of a correct sequence/conformation of loop 113–119 in the cooperative phenomenon. As shown in Table 2, this loop is crucially involved in intersubunit communication; in fact, all mutants in the presence of GSH bind hemin with a noncooperative modality. Furthermore they display an affinity for hemin similar to that of wild type in the high affinity state.

*GSH Is Not Essential for Hemin Binding—Pf*GST is able to bind hemin only when the enzyme is in the active dimeric structure, *i.e.* in complex with GSH (15). Because of the fast tetramerization of the enzyme in the absence of GSH, it remains uncertain whether the hemin binding is prevented by steric hindrance caused by the tetrameric structure or by the absence of GSH in the G-site. The particular inertness of the mutated enzymes makes it possible to clarify this question. Binding of hemin has been visualized on the basis of the quenching of intrinsic fluorescence. The results, reported in Table 3 and Fig. 5, indicate that all mutants are able to bind hemin in the absence of GSH. However, the affinity is lower than that shown by the GSH·enzyme complex. It appears that all of these mutants display two different states characterized by two different affinities for hemin, one high affinity conformation, R-state (relaxed state), and one low affinity conformation, T-state (tensed state), determined by the presence or absence of GSH. The ability of loop 113–119 to adopt different conformations is possibly linked to this high-low affinity transition for hemin binding. Because Asn-112 is involved in the hemin stabilization through coordination to the iron atom (15), it is not surprising that any structural change of loop 113–119 may cause such relevant effects for the hemin binding. The model for hemin-associated *Pf*GST reported in Fig. 1*B* (15) shows the close proximity of loop 113–119 with the bound hemin that also contacts the adjacent subunit. These contacts could represent the structural basis for cooperativity. Importantly, we also observed that the native enzyme is able to bind hemin also in the presence of GSSG. In this case the binding is noncooperative, and the dissociation constant indicates a low affinity con-

TABLE 2

Binding of hemin to *Pf*GSTs and human GSTs calculated from inhibition data

Shown are the inhibition data fitted to the Hill equation $v_i/v_{max} = [S]^n/(K^n + [S]^n)$. hGST, human GST.

*Pf*GST	n_H	$K_{D\,app}$
		μM
Wild-type[a]	1.9 ± 0.1	2.8 (K_1, low affinity), 0.16 (K_2, high affinity)
Mutant A (hinge-blocked)	1.2 ± 0.2	0.46 ± 0.03
Mutant B (point mutation)	1.1 ± 0.1	0.15 ± 0.01
Mutant C (mini loop)	1.0 ± 0.1	0.22 ± 0.02
hGSTP1-1	1.1 ± 0.1	0.10 ± 0.02
hGSTA1-1	1.0 ± 0.2	0.060 ± 0.003
hGSTM2-2	1.0 ± 0.1	0.11 ± 0.02

[a] The data are from Ref. 15 where K_1 and K_2 were obtained by fitting experimental data to the Adair equation.

TABLE 3

Isothermic binding of hemin to *Pf*GSTs

*Pf*GST	K_D[a]
	μM
Wild-type	
1 mM GSSG	1.9 ± 0.1
0.01 mM GSSG	1.5 ± 0.2
Mutant A (hinge-blocked)	
5 mM GSH	<0.1
—[b]	1.3 ± 0.1
Mutant B (point mutation)	
1 mM GSH	<0.1
—	0.9 ± 0.1
Mutant C (mini loop)	
1 mM GSH	<0.1
—	1.9 ± 0.1

[a] K_D values were determined by fitting the experimental data to Equation 3. No cooperativity has been observed for wild type in the presence of GSSG and for all mutants in the absence of GSH.
[b] —, no GSH added.

formation (Table 3 and Fig. 5). This behavior parallels what was observed in the presence of *S*-methylglutathione (15) and indicates that the free thiol group in the active site is important for the cooperative mechanism and to shift the enzyme toward a high affinity state. The ability of *Pf*GST to bind hemin in the presence of GSSG may be of physiological relevance because this enzyme would protect the cell from hemin even under severe oxidative stress conditions. The model in Scheme 1 is consistent with all of the results described above.

Concluding Remarks—A few structural and functional properties of *Pf*GST make this enzyme unique in the wide scenario of GSTs in living organisms. One of these is the peculiar tetramerization that parallels the complete inactivation of the enzyme and that occurs in a few minutes in the absence of GSH (15). The present results show these events to be very slow when selected mutations have been introduced in loop 113–119. Thus, the integrity of this loop is crucial for a fast tetramerization/inactivation process. The possible physiological impact of the tetramerization process *in vivo* obviously depends on the glutathione levels present in the parasite. It has been shown that the GSH concentration in *P. falciparum* may vary from 0.2 to 2.6 mM, depending on the parasite strain and possibly also on the stage in the life cycle (26–28). Given that the tetramerization event occurs within the GSH range of 0–0.7 mM, it seems likely that the physiological level of glutathione might regulate the activity of this enzyme *in vivo*. The data reported here demonstrate that not only GSH but even GSSG is able to slow down inactivation drastically. Thus, the tetramerization is not driven by the redox status of the parasite but only by the total level of glutathione.

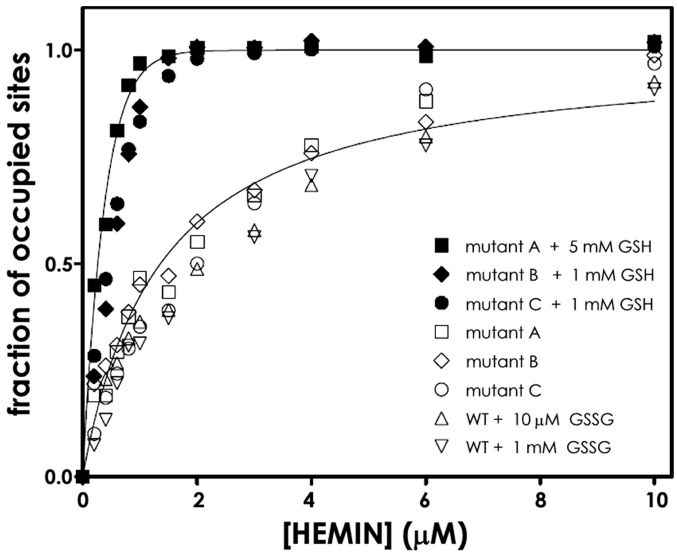

FIGURE 5. **Isothermic binding of hemin to wild-type and mutant *Pf*GSTs as determined by fluorescence quenching.** Hemin was added to *Pf*GSTs (1 μM) in the presence or absence of GSH or GSSG in 0.1 M potassium phosphate buffer, pH 6.5, 25 °C. Quenching of the intrinsic fluorescence was measured as described under "Experimental Procedures," and the data were analyzed by Equations 3 and 4. The *continuous lines* represent global fits to the high affinity and low affinity data, respectively. *WT*, wild type.

The peculiar loop 113–119 is also deeply involved in the hemin binding and in particular in the cooperative phenomenon that characterizes this interaction. In fact, the positive homotropic behavior triggered by hemin itself (15) disappears completely when this loop is truncated, stiffened, or slightly modified by a single point mutation (Table 2). Furthermore, the presence of GSH in the G-site is not essential for hemin binding. In particular, in the absence of GSH, all mutated enzymes show a low affinity state for hemin and noncooperative binding (Table 3 and Fig. 5). Interestingly, a shift toward a high affinity conformation for hemin binding is triggered by GSH in all mutants but not in the native enzyme, where both subunits remain in the low affinity conformation until one hemin molecule binds to one subunit.

From a more general point of view, the present data also yield new physiological suggestions for this peculiar cooperativity. In fact, it has previously been suggested that the affinity of the enzyme must be increased in cases with toxic levels of hemin (15). However, this idea must be revised. We must keep in mind that many GSTs bind hemin efficiently, and in the case of Alpha, Mu, and Pi isoenzymes, binding is noncooperative and has an affinity similar to that of the high affinity state of *Pf*GST (Table 2). In addition, a stronger hemin binding by *Pf*GST can be easily obtained during evolution even by a simple point mutation, as demonstrated for our mutants (Table 2). Thus, it is unlikely that the evolution pressure for this enzyme simply

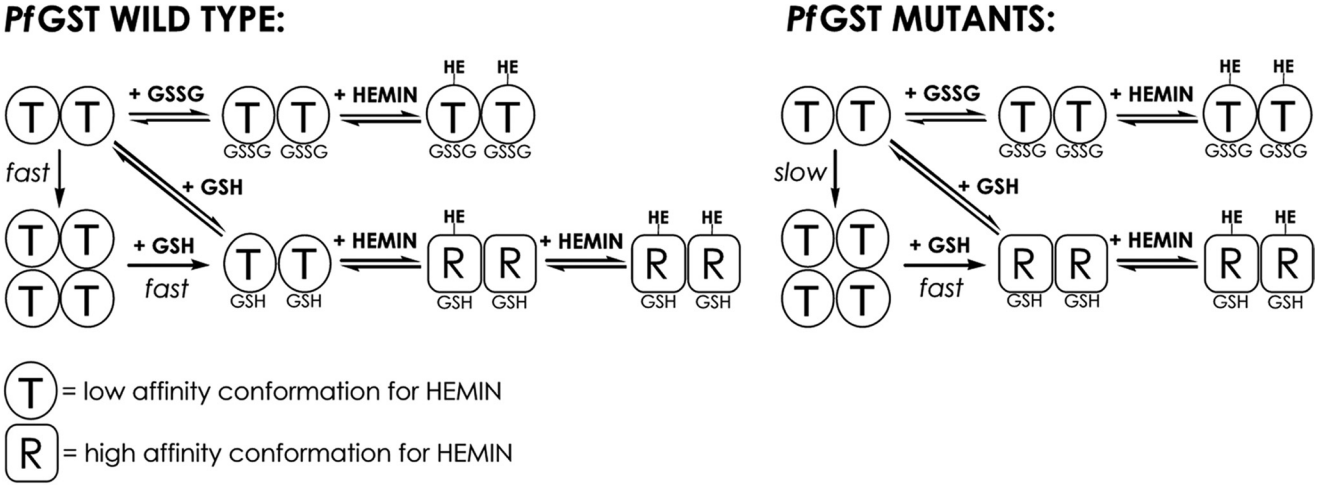

SCHEME 1

pushed it toward a higher affinity for hemin. On the contrary, it seems possible that this particular type of cooperativity may have evolved to confer lower affinity at low (nontoxic) hemin levels and higher affinity at higher (toxic) hemin concentrations. This explanation is plausible considering that the parasite lives in the erythrocyte, that it is likely exposed to free hemin, and that the *Pf*GST is completely inactivated when hemin is bound. In other terms, because of the particular environment of *Plasmodium*, this enzyme could have evolved to preserve catalytic detoxifying activity as long as the free hemin level is harmless to the parasite. Although for a very different purpose, this is reminiscent of the development of hemoglobin, which evolved from an ancestral globin at high affinity to become the tetrameric cooperative protein that promotes oxygen release at the tissue level when shifted toward a lower affinity conformation.

Such a cooperative mechanism in *Pf*GST is also consistent with the idea that a low amount of free hemin may have a regulatory function in *P. falciparum* by inhibiting glyceraldehyde-3-phosphate dehydrogenase and promoting the metabolism of glucose through the hexose monophosphate shunt (12, 29). This pathway provides NADPH as a reducing fuel that counteracts possible oxidative stress. In any case, the identification of the peculiar loop 113–119 as the crucial determinant of the cooperative hemin binding makes this protein segment of particular interest as an antimalarial drug target.

REFERENCES

1. Breman, J. G. (2001) *Am. J. Trop. Med. Hyg.* **64,** 1–11
2. Greenwood, B., and Mutabingwa, T. (2002) *Nature* **415,** 670–672
3. Salinas, A. E., and Wong, M. G. (1999) *Curr. Med. Chem.* **6,** 279–309
4. Sheehan, D., Meade, G., Foley, V. M., and Dowd, C. A. (2001) *Biochem. J.* **360,** 1–16
5. Deponte, M., and Becker, K. (2005) *Methods Enzymol.* **401,** 241–253
6. Adler, V., Yin, Z., Fuchs, S. Y., Benezra, M., Rosario, L., Tew, K. D., Pincus, M. R., Sardana, M., Henderson, C. J., Wolf, C. R., Davis, R. J., and Ronai, Z. (1999) *EMBO J.* **18,** 1321–1334
7. Pedersen, J. Z., De Maria, F., Turella, P., Federici, G., Mattei, M., Fabrini, R., Dawood, K. F., Massimi, M., Caccuri, A. M., and Ricci, G. (2007) *J. Biol. Chem.* **282,** 6364–6371
8. Mannervik, B., and Danielson, U. H. (1988) *CRC Crit. Rev. Biochem.* **23,** 283–337
9. Meyer, D. J., Coles, B., Pemble, S. E., Gilmore, K. S., Fraser, G. M., and Ketterer, B. (1991) *Biochem. J.* **274,** 409–414
10. Pemble, S. E., Wardle, A. F., and Taylor, J. B. (1996) *Biochem. J.* **319,** 749–754
11. Board, P. G., Baker, R. T., Chelvanayagam, G., and Jermiin, L. S. (1997) *Biochem. J.* **328,** 929–935
12. Harwaldt, P., Rahlfs, S., and Becker, K. (2002) *Biol. Chem.* **383,** 821–830
13. Fritz-Wolf, K., Becker, A., Rahlfs, S., Harwaldt, P., Schirmer, R. H., Kabsch, W., and Becker, K. (2003) *Proc. Natl. Acad. Sci. U.S.A.* **100,** 13821–13826
14. Becker, K., Tilley, L., Vennerstrom, J. L., Roberts, D., Rogerson, S., and Ginsburg, H. (2004) *Int. J. Parasitol.* **34,** 163–189
15. Liebau, E., De Maria, F., Burmeister, C., Perbandt, M., Turella, P., Antonini, G., Federici, G., Giansanti, F., Stella, L., Lo Bello, M., Caccuri, A. M., and Ricci, G. (2005) *J. Biol. Chem.* **280,** 26121–26128
16. Tripathi, T., Rahlfs, S., Becker, K., and Bhakuni, V. (2007) *BMC Struct. Biol.* **7,** 67–76
17. Hiller, N., Fritz-Wolf, K., Deponte, M., Wende, W., Zimmermann, H., and Becker, K. (2006) *Protein Sci.* **15,** 281–289
18. Perbandt, M., Burmeister, C., Walter, R. D., Betzel, C., and Liebau, E. (2004) *J. Biol. Chem.* **279,** 1336–1342
19. Liebau, E., Bergmann, B., Campbell, A. M., Teesdale-Spittle, P., Brophy, P. M., Lüersen, K., and Walter, R. D. (2002) *Mol. Biochem. Parasitol.* **124,** 85–90
20. Müller, S., Liebau, E., Walter, R. D., and Krauth-Siegel, R. L. (2003) *Trends Parasitol.* **19,** 320–328
21. Gill, S. C., and von Hippel, P. H. (1989) *Anal. Biochem.* **182,** 319–326
22. Lo Bello, M., Nuccetelli, M., Caccuri, A. M., Stella, L., Parker, M. W., Rossjohn, J., McKinstry, W. J., Mozzi, A. F., Federici, G., Polizio, F., Pedersen, J. Z., and Ricci, G. (2001) *J. Biol. Chem.* **276,** 42138–42145
23. Board, P. G., and Pierce, K. (1987) *Biochem. J.* **248,** 937–941
24. Ross, V. L., and Board, P. G. (1993) *Biochem. J.* **294,** 373–380
25. Lakowicz, J. R. (2006) *Principles of Fluorescence Spectroscopy*, pp. 353–382, Springer, New York
26. Meierjohann, S., Walter, R. D., and Müller, S. (2002) *Biochem. J.* **368,** 761–768
27. Atamna, H., and Ginsburg, H. (1997) *Eur. J. Biochem.* **250,** 670–679
28. Lüersen, K., Walter, R. D., and Müller, S. (2000) *Biochem. J.* **346,** 545–552
29. Campanale, N., Nickel, C., Daubenberger, C. A., Wehlan, D. A., Gorman, J. J., Klonis, N., Becker, K., and Tilley, L. (2003) *J. Biol. Chem.* **278,** 27354–27361

Enzyme Catalysis and Regulation:

Tetramerization and Cooperativity in *Plasmodium falciparum* Glutathione *S*-Transferase Are Mediated by Atypic Loop 113 –119

Eva Liebau, Kutayba F. Dawood, Raffaele Fabrini, Lena Fischer-Riepe, Markus Perbandt, Lorenzo Stella, Jens Z. Pedersen, Alessio Bocedi, Patrizia Petrarca, Giorgio Federici and Giorgio Ricci

J. Biol. Chem. 2009, 284:22133-22139.
doi: 10.1074/jbc.M109.015198 originally published online June 16, 2009